

**Tests of internal-conversion theory with precise  $\gamma$ - and x-ray spectroscopy:  
The case of  $^{127m}\text{Te}$**

N. Nica, K. Brandenburg, J. C. Hardy, V. E. Jacob, H. I. Park, and M. B. Trzhaskovskaya<sup>1</sup>  
<sup>1</sup>*Petersburg Nuclear Physics Institute, Gatchina RU-188300, Russia*

Internal conversion is an important component of most nuclear decay schemes. In order to balance decay schemes correctly, one needs to know the internal conversion contribution to each transition as expressed by its internal conversion coefficient (ICC). Nevertheless, ICCs are only rarely measured; instead they are taken from tabulations. As a result, calculated ICCs are essential input to every decay scheme, except those for the lightest nuclei. Unfortunately, over the decades, tabulated ICC values have differed significantly from one calculation to another by a few percent. Although for many applications such differences can be tolerated, transitions used in critical calibrations require very precise and accurate ICC values, precision that has simply been impossible to guarantee at the one-percent level or below.

In order to correct for this deficiency one can only seek guidance from measured ICCs that have sufficient precision to distinguish among the various calculations. However, as recently as about a decade ago, when a survey of measured ICCs was made by Raman et al. [1], there were only five published ICC values with precision of the order of  $\pm 1\%$ , not enough to make any definitive conclusion possible. At that time, one aspect of the ICC calculations remained a particular concern. The final-state electron wave function must be calculated in a field that adequately represents the remaining atom. But should that representation include the atomic vacancy created by the conversion process? Some calculations included it and some did not.

Thus the problem of measuring ICCs at the  $\pm 1\%$  precision level became critical and, with our very precisely efficiency-calibrated HPGe detector [2], we found ourselves in a position to be able to address it. Consequently, over the past decade we have been measuring a series of ICCs [3,4] covering a wide range of atomic numbers,  $50 \leq Z \leq 78$ . So far, all these results have indicated that the atomic vacancy should be taken into account in the calculations. With  $Z = 52$ , the new case reported here – an 88.2-keV  $M4$  transition in  $^{127}\text{Te}$  – lies in the lower end of that range.

As can be seen from Fig. 1, the 88.2-keV  $M4$  transition in  $^{127}\text{Te}$  is an isolated transition that converts in the atomic  $K$  shell. For such a transition, the observation of a  $K$  x ray is a signal that an electron conversion has taken place; whereas a  $\gamma$  ray indicates that no conversion has taken place. If both x rays and  $\gamma$  rays are recorded in a measurement, then the value of  $\alpha_K$  is given by

$$\alpha_K \omega_K = \frac{N_K}{N_\gamma} \cdot \frac{\epsilon_\gamma}{\epsilon_K} \quad (1)$$

where  $\omega_K$  is the fluorescence yield, which we take from Ref. [5];  $N_K$  and  $N_\gamma$  are the respective peak areas of the  $K$  x rays and the  $\gamma$  ray; and  $\epsilon_K$  and  $\epsilon_\gamma$  are the corresponding detector efficiencies. As described in Ref. [2], the  $\epsilon_\gamma$  for an 88.2-keV  $\gamma$  ray in our detector is known to  $\pm 0.15\%$  relative precision; however a special investigation was required in order to get a precise value for  $\epsilon_K$  at the  $\sim 28$ -keV energy of the Te  $K$  x rays.

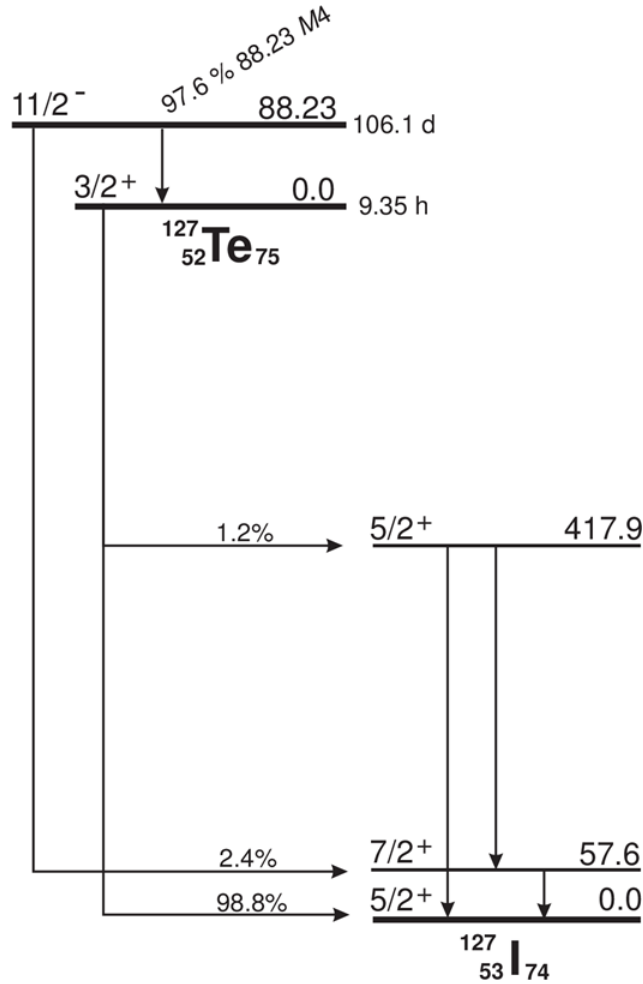


**FIG. 1.** Decay scheme of the ground and isomeric state in  $^{127}\text{Te}$ . Very weak beta branches have been left out for clarity.

We produced a source of  $^{127m}\text{Te}$  by neutron activation of  $^{126}\text{Te}$ . Tellurium is an element with eight stable isotopes:  $^{120}\text{Te}$  (0.09%),  $^{122}\text{Te}$  (2.55%),  $^{123}\text{Te}$  (0.89%),  $^{124}\text{Te}$  (4.74%),  $^{125}\text{Te}$  (7.07%),  $^{126}\text{Te}$  (18.84%),  $^{128}\text{Te}$  (31.74%), and  $^{130}\text{Te}$  (34.08%). Even though  $^{126}\text{Te}$  is one of the more abundant isotopes, we could not use natural tellurium for activation since the other tellurium isotopes produce radiation, particularly x rays, which interfere with those emitted by  $^{127m}\text{Te}$  itself. For this reason we procured  $^{126}\text{Te}$ , 98.8% enriched, from Trace Sciences International. Nevertheless, even the small concentrations of other tellurium isotopes that remained produced some interference in the  $K$  x ray region of the spectrum.

As delivered, our  $^{126}\text{Te}$  material was in the form of metal powder with a grain size of  $25\pm 5$  microns. We ground this powder until its grain size was less than 1 micron, as determined by our observing the grains with a microscope. A 12-micron tungsten wire placed in the visual field was used for reference. An amount of about 1.3 mg of this powder was spread uniformly in a 10-mm-diameter layer, about 2 microns thick, held between two thin Mylar films. This sample was activated for 24 h at the Texas A&M Nuclear Science Center TRIGA reactor, in a thermal neutron flux of  $7.5\times 10^{12}$  neutron/( $\text{cm}^2\text{s}$ ). An identical “blank” sample (only Mylar with no  $^{126}\text{Te}$ ) was also activated together with the real sample, so as to establish the impurities that come from the activation of Mylar.

After the activation was completed the sources were kept for one month to allow the short-lived impurities to decay. This was especially necessary to remove the 2.7-d activity from  $^{122}\text{Sb}$ , which is strongly present in activated Mylar. When we prepared the  $^{127\text{m}}\text{Te}$  source for measurement with the HPGe detector we found that it was no longer flat, but was curled into a small rolled cylinder. Because the Mylar had become brittle after activation, the sample cracked as we unrolled it and about one quarter of the tellurium powder was lost. The partially unrolled source was then sealed between two additional thin Mylar foils. After this repair the source was twice as thick as the unbroken initial one. The extra thickness was accounted for when we later calculated the relative attenuation of the K x rays and  $\gamma$  rays in the sample.

The repaired source was placed at our standard distance of 151 mm from the face of our well-calibrated HPGe detector and a spectrum was recorded continuously for about one month. A 24-h spectrum was also acquired from the blank Mylar source. The only remaining impurity we observed coming from Mylar was  $^{124}\text{Sb}$ , which  $\beta^-$ -decays to  $^{124}\text{Te}$  and, through subsequent internally-converted transitions, leads to the emission of Te x rays. These had to be corrected for in our analysis of the  $^{127\text{m}}\text{Te}$  decay.

As shown in Fig. 1, the 88.2-keV, 106.1-d metastable state in  $^{127}\text{Te}$  decays 97.6% by the *M4* transition we are interested in here. The remaining 2.4% of the state’s decay is via  $\beta^-$ -decay to  $^{127}\text{I}$ . Furthermore, the  $^{127}\text{Te}$ , 9.4-h ground state, which is populated by the *M4* transition, also decays by  $\beta^-$  to  $^{127}\text{I}$ . Both these decay branches produce, through subsequent internally-converted transitions in  $^{127}\text{I}$ , iodine K x rays, which overlap the tellurium x rays of interest. The contributions that these two decays made to the tellurium x-ray energy region were: 3.5(6)% from the metastable state decay and 0.226(15)% from the ground-state decay. The other sources of impurity contributing to the same energy region were:  $^{125\text{m}}\text{Te}$  2.63(6)%,  $^{129\text{m}}\text{Te}$  0.309(12)%,  $^{129}\text{Te}$  0.12(5)%,  $^{123\text{m}}\text{Te}$  0.104(3)%,  $^{131}\text{I}$  0.0374(9)%,  $^{121}\text{Te}$  0.0171(12)%,  $^{124}\text{Sb}$  0.0144(3)% and  $^{110\text{m}}\text{Ag}$  0.000487(11)%. Thus, the total contribution to the K x-ray energy region from activities other than the *M4* decay of  $^{127\text{m}}\text{Te}$  amounted to about 7%. A small 0.081(3)% impurity (coming from the 88.5-keV  $\gamma$  ray from  $^{123\text{m}}\text{Te}$ ) affected the 88.2-keV  $\gamma$  ray.

Some of the photons from a radioactive source scatter from nearby materials - including air - in the vicinity of the detector setup and, entering the detector, they form a continuum in the energy spectrum extending to lower energy from the peak created by unscattered photons. For photons above  $\sim 50$  keV this continuum is rather flat and extends to energies well below the corresponding peak so, by extrapolation, its contribution to the area of the peak can easily be determined and removed. However, for peaks with energies as low as 27.4 keV and 31.1 keV, the energies of the tellurium  $\text{K}_\alpha$  and  $\text{K}_\beta$  x rays respectively, the

continuum is more like a shelf that extends only 2-3 keV below the peak energy. At our energy resolution of  $\sim 1$  keV in this region, an important part of the continuum gets "hidden" in, and potentially counted together with, the peak itself. The number of counts in the "hidden" continuum is very dependent not only on the source-detector geometry, but also on the details of its neighborhood. For this reason it is impossible to define a universal efficiency calibration with useful precision below  $\sim 50$  keV. Rather, one must examine each geometry as a special case, which must be calibrated based on its specific properties.

For our previously measured  $\alpha_K$  case in  $^{119m}\text{Sn}$  [4] we followed two different approaches to this part of the analysis. In the first, described fully in our paper on  $^{134}\text{Cs}$  and  $^{137}\text{Ba}$  [3], we employed Monte Carlo calculations with the CYLTRAN code - the same code used in our calibration procedures [2] - to simulate the scattering "shelf"; then we scaled up the result to match the small component of the shelf visible in the data; and finally used that scaled-up result to determine the component of the shelf contained within the peak.

Our second approach in Ref. [4] was to measure a calibration source,  $^{109}\text{Cd}$ , which decays by electron capture to  $^{109}\text{Ag}$  followed by the emission of a unique 88.0-keV M4  $\gamma$  transition. The K x rays of silver, following both the electron capture decay and the electron conversion of the 88.0-keV transition, form prominent x-ray groups situated at 22.1 keV ( $K_\alpha$ ) and 25.0 keV ( $K_\beta$ ). The K x-rays together with the 88.0 keV  $\gamma$  ray can be used with a formula similar to eq. (1) to deduce  $\epsilon_K$  at silver K x-ray energies if we use calculated  $\alpha_K$  values for the 88.0-keV transition in  $^{109}\text{Ag}$ . By taking the mean value of calculated 'vacancy' and 'no vacancy'  $\alpha_K$  values with an uncertainty encompassing both, we obtain an  $\alpha_K$  value that is independent of the treatment of the atomic vacancy. Then by a short interpolation from silver K x-ray energies to tellurium K x-ray energies, we can arrive at  $\epsilon_K$  values for tellurium with a total uncertainty of about  $\pm 1\%$ .

For  $^{119m}\text{Sn}$ , the result obtained by this method was in very good agreement (within 0.3%) with the CYLTRAN-based value, giving us confidence in this methodology to correct for scattering effects. We have used the same procedure in the case of  $^{127m}\text{Te}$ .

The preliminary result we report here for the 88.2-keV, M4 transition from  $^{127m}\text{Te}$  is  $\alpha_K = 489(7)$  which compares well with the 'hole' calculation in the "frozen orbital" approximation (486.4), and disagrees with the 'no hole' calculation (468.6). Our new result confirms and strengthens our conclusion that the atomic vacancy created by the internal conversion process must be taken into account when calculating ICCs.

- [1] S. Raman *et al.*, Phys. Rev. C **66**, 044312 (2002).
- [2] J.C. Hardy *et al.*, Appl. Radiat. Isot. **56**, 65 (2002) ; R.G. Helmer *et al.*, Nucl. Instrum. Methods Phys. Res. **A511**, 360 (2003); R.G. Helmer *et al.*, Appl. Radiat. Isot. **60**, 173 (2004).
- [3] N. Nica *et al.*, Phys. Rev. C **70**, 054305 (2004); Phys. Rev. C **71**, 054320 (2005); N. Nica *et al.*, Phys. Rev. C **75**, 024308 (2007); Phys. Rev. C **77**, 034306 (2008) ; Phys. Rev. C **80**, 064314 (2009).
- [4] N. Nica *et al.*, Phys. Rev. C **89**, 014303 (2014); J.C. Hardy *et al.*, Appl. Radiat. Isot. **87**, **87** (2014).
- [5] E. Schönfeld and H. Janssen, Nucl. Instrum. Methods Phys. Res. **A369**, 527 (1996).